ORIGINAL RESEARCH

Preparation and characterization of vinculin-targeted polymer–lipid nanoparticle as intracellular delivery vehicle

Junping Wang*
Ceren Örnek-Ballanco*
Jiahua Xu
Weiguo Yang
Xiaojun Yu

Department of Chemistry, Chemical Biology, and Biomedical Engineering, Stevens Institute of Technology, Hoboken, NJ, USA

*These authors contributed equally to this work

Abstract: Intracellular delivery vehicles have been extensively investigated as these can serve as an effective tool in studying the cellular mechanism, by delivering functional protein to specific locations of the cells. In the current study, a polymer–lipid nanoparticle (PLN) system was developed as an intracellular delivery vehicle specifically targeting vinculin, a focal adhesion protein associated with cellular adhesive structures, such as focal adhesions and adherens junctions. The PLNs possessed an average size of 106 nm and had a positively charged surface. With a lower encapsulation efficiency 32% compared with poly(lactic-co-glycolic) acid (PLGA) nanoparticles (46%), the PLNs showed the sustained release profile of model drug BSA, while PLGA nanoparticles demonstrated an initial burst-release property. Cell-uptake experiments using mouse embryonic fibroblasts cultured in fibrin–fibronectin gels observed, under confocal microscope, that the anti-vinculin conjugated PLNs could successfully ship the cargo to the cytoplasm of fibroblasts, adhered to fibronectin–fibrin. With the use of cationic lipid, the unconjugated PLNs were shown to have high gene transfection efficiency. Furthermore, the unconjugated PLNs had nuclear-targeting capability in the absence of nuclear-localization signals. Therefore, the PLNs could be manipulated easily via different type of targeting ligands and could potentially be used as a powerful tool for cellular mechanism study, by delivering drugs to specific cellular organelles.

Keywords: 3D gel, PLGA, targeting

Introduction

Due to their nano size (10–1000 nm), biocompatibility, and versatility, nanoparticles have been widely investigated for various biomedical applications, such as drug delivery,[1] gene transfer,[2,3] and cancer diagnosis.[4] Nanoparticles made from biodegradable polymers are one potential system for delivery of active payloads, and several biodegradable polymers, such as polylactic acid (PLA), polyglycolic acid (PGA), and their copolymers, poly(lactic-co-glycolic) acid (PLGA) and polycaprolactone (PCL), have been used for the fabrication of nanoparticle-based carriers.[5–7] Polymeric nanoparticles are preferred over other colloidal carrier systems, like micelles, owing to their higher stability and flexibility in tailoring the drug load and release rate.

Nanoparticles coupled with targeting ligands allow the drug-loaded delivery system to target certain cell types or cell organelles via the interaction with specific cell-surface or cell-organelle proteins, which significantly reduces the side effects of the drug. In order to achieve a specific therapeutic effect, some drugs have to be targeted to specific cell organelles,[8] for example, mitochondria-targeting of antiapoptotic drugs[9] and lysosome-targeting of drugs[10] for lysosomal storage-disorder diseases.

Correspondence: Xiaojun Yu
Department of Chemistry, Chemical Biology and Biomedical Engineering, Stevens Institute of Technology, Hoboken, NJ, 07030, USA
Tel +1 201 216 5256
Fax +1 201 216 8306
Email xyu@stevens.edu

In addition, the intracellular targeting nanoparticles could be a very effective tool for studying the cellular mechanism, by delivering functional protein to specific locations of the cells. Nanoparticles used for this purpose have to overcome the obstacles of endosome entrapment and lysosome degradation[11] to reach the appropriate cellular compartment after endocytosis.[12,13] For example, nanoparticles for DNA delivery must escape endosomal–lysosomal degradation to ensure DNA enters the nuclei for gene transcription after cellular uptake.[14]

Successful intracellular targeting delivery includes three steps: firstly, cellular uptake via receptor-mediated endocytosis; secondly, for most nonlysosomal targeting delivery, nanoparticles have to be able to escape the acidic endosomal–lysosomal compartment to avoid being digested; thirdly, nanoparticles could finally be localized by the cellular organelle-targeting ligands. The first step could be easily achieved via the control of nanoparticle size and surface chemistry. It has been reported that the smaller the particle, the easier it can be delivered to cells.[15] A range of 50–200 nm was suggested by Mailänder and Landfester[16] for efficient nanoparticle-mediated delivery. A cationic polymer coating, such as polyethylenimine or chitosan, has also been shown to enhance the cellular uptake significantly.[17,18] The second step requires the use of polymers with endosomal–lysosomal escape properties. The most frequently used are endosomolytic polycationic polymers such as PEI, which commonly serve as a nonviral gene-delivery vector. The release of this type of polyplexes after cellular uptake could be explained by the proton sponge hypothesis[19] and the increasing electrostatic repulsion of charged groups in the acidic lysosome compartment.[20] With the same electrostatic repulsion principle, pH-responsive polymer has also been employed as an intracellular protein transporter.[21] A solution for the third step is the linkage of nanoparticles with specific targeting ligands, which are usually antibody-specific to certain cellular organelles.

Several studies have reported intracellular targeting of nanoparticles composed of silica, quantum dots, and carbon nanotubes.[22] PLGA nanoparticles (PLGA-NPs) have been reported to deliver plasmid DNA into macrophages, a phagocytic cell type.[23] We figured that development of biodegradable nanoparticles capable of intracellular targeting and sustained cargo release will have both clinical and biomedical research advantage. Therefore, this study aimed to investigate an anti-vinculin coupled polymer-lipid nanoparticle (PLN) system for intracellular delivery of functional proteins to specific organelles of the cells – the focal adhesion site of cells. Vinculin, a highly conserved focal adhesion protein, is localized on the cytoplasm surface of cell–extracellular matrix junctions, also called focal adhesions and cell–cell junctions.[24] It is a key protein regulating the transmission of contractile forces between the environment and cytoskeleton.[25,26]

Specifically, PLGA, an FDA-approved biodegradable and biocompatible polymer, was adopted for preparing the nanoparticle. In order to achieve a high delivery efficacy of the PLNs to cells, a cationic lipid was used as the surface coating material of PLN, aiming to facilitate cellular uptake of PLNs via charge interaction. Tween® 80 here acted both as a surfactant to promote the formation of PLNs and as a stabilizer to avoid aggregation of PLNs. Antibody against vinculin was further conjugated to PLNs carrying bovine serum albumin (BSA) as cargo.

Materials and methods
Materials
All solutions were prepared with distilled and deionized water. All chemicals were obtained from Sigma-Aldrich (St Louis, MO), unless otherwise specified.

Preparation of PLNs
The new formulation of cationic PLN was constructed by the traditional double emulsion technique.[27] Briefly, the first emulsion was obtained by adding the water phase containing 100 µL of 10 mg/mL BSA or Texas Red-labeled BSA to the oil phase containing 1 mL of 1% (w/v) PLGA (85:15) (Lakeshore Biomaterials Inc, Birmingham, AL) in dichloromethane and then emulsifying the solution in an ice-water bath, using a high-intensity probe ultrasonicator, for 15 seconds at 25 w. The mixture was then poured into 10 mL of a second water phase containing DC-Cholesterol, Tween 80, DOTAP, and DSPE: PEG2000:Maleimide (Avanti Polar Lipids Inc, Alabaster, AL) at the concentration of 0.3 mg/mL, using sonication for 1 minute at 25 w. A magnetic stir was then put into the emulsion to evaporate the organic solvent. After overnight evaporation, the PLN suspension was formed. The PLNs were then collected by centrifuge. Unabsorbed BSA was washed with deionized water by ultracentrifuge (11,000 rpm, 15 minutes). All the supernatant was collected for the encapsulation efficiency measurement. PLGA-NPs (without the lipid layer) were also fabricated as the control for the delivery system, using the same methods mentioned above; instead of using the lipid mixture as the second water phase, 1% (w/v) polyvinyl alcohol solution was used as the surfactant for the formation of PLGA-NPs.

Preparation of anti-vinculin–fluorescein isothiocyanate (FITC)-conjugated PLNs

The anti-vinculin-FITC was added to the PLN at 0.13 mg of protein per each 10 μmol of DSPE: PEG2000:Maleimide and incubated at pH 7.3–7.4 (NaOH) for 2 hours at room temperature, under inert atmosphere. The reaction was stopped by blocking excess maleimido groups with 2 mM b-mercaptoethanol. Unconjugated protein was removed by using a standard RC membrane (molecular weight cut-off [MWCO]: 12,000–14,000 Daltons) for 48-hour dialysis.

Characterization of PLNs

PLNs were gold coated for 25 seconds and examined for shape and morphology using a scanning electron microscope (SEM) (Leo 982 FEG-SEM; Carl Zeiss SMT Inc, Jena, Germany). The size distribution of PLNs was measured by laser light scattering. For particle size analysis of the complexes, the complexes were diluted with deionized water within a water bath sonicator, in order to form a uniform suspension prior to size measurement. The zeta potential of complexes was analyzed using the same equipment, at room temperature.

Encapsulation efficiency and in vitro release study

After being centrifuged, the supernatant of PLNs was collected, and the BSA concentration of this solution was detected using a Bio-Rad Protein Assay Kit I (#500-0001; Bio-Rad Laboratories, Hercules, CA). The encapsulation efficiency was calculated as the percent weight of BSA present in nanocarriers relative to the weight of BSA used for formulation. After being freeze-dried, the protein-loaded PLNs were used for a 6-day release study. Briefly, 5 mg of PLNs in 1 mL of phosphate-buffered saline (PBS) was put in a 37°C water bath, and a sample was collected every day in order to detect the amount of protein released (using the Bio-Rad assay kit). The amount of drug released with time was expressed as a percent of the initial drug loaded in the PLN.

Cell lines

Mouse embryo fibroblasts (MEFs) were adopted as model cells for cellular uptake and localization of the PLNs. Cells were maintained in medium containing Dulbecco's modified Eagle medium (DMEM) supplemented with antibiotic solution (1% penicillin–streptomycin), and 10% FBS (HyClone® FBS; Thermo Fisher Scientific, Waltham, MA).

Human osteoblast cells (hFOB 1.19; American Type Culture Collection [ATCC], Manassas, VA) were adopted as model cells for the preliminary evaluation of the endosomal–lysosomal escape property of PLNs. Cells were cultured in medium containing a 1:1 mixture of Ham's F12 medium (Life Technologies, Carlsbad, CA) and DMEM supplemented with antibiotic solution (1% penicillin–streptomycin), and 10% FBS. All the cells were maintained in a humidified atmosphere of 5% CO_2 at 37°C.

Cellular uptake of nanoparticles

Texas Red-labeled BSA (TR-BSA) was used for this study, to evaluate the cellular uptake of nanoparticles. The nanoparticles used for this study were TR-BSA (control group), PLGA-NPs with TR-BSA loading, and PLNs with TR-BSA loading. MEF cells were seeded on an 8-well chamber and cultured overnight. After that, cell monolayers were incubated with 1 mg/mL of nanoparticles or BSA only, in cell culture medium for 4 hours. After incubation, excessive nanoparticles or TR-BSA were removed by PBS rinse. The cells were then fixed with 4% paraformaldehyde for 20 minutes and then washed with PBS three times. Fluorescent microscopy was applied to visualize the TR-BSA loaded within nanoparticles (LSM 510 Meta; Carl Zeiss).

Transfection with PLNs

The purpose of this study was to evaluate the endosomal–lysosomal escape capacity of cationic PLNs by using gene transfection assay. pIRS-EGFP (Clontech Laboratories Inc, Mountain View, CA) was used in this study. Human osteoblast cells were seeded on the cover glass with a 24-well plate one night before the transfection experiment. Expressed green fluorescent protein (GFP) was visualized by confocal microscopy 24 hours after transfection. Lipofectamine™ 2000 (Life Technologies) was used as the control for the assay, to evaluate the gene transfection efficiency of PLNs.

Results and discussion
Characterization of PLNs

PLNs were successfully prepared via the double emulsion technique as shown in Figure 1. The resultant PLNs were nanospheres with uniform size range, and aggregation or clogs of PLNs was not observed in the SEM morphology study. Laser light-scattering was used to measure the particle size of two groups: PLNs and conventional PLGA-NPs (control group). As demonstrated in Table 1, these two groups of PLGA-based nanoparticles, which were fabricated by same technique, possessed significantly different particle size. PLNs possessed a smaller particle size, with an average size of 106 nm, while conventional PLGA NPs have an average of 209 nm. It has been reported that nanoparticle size was
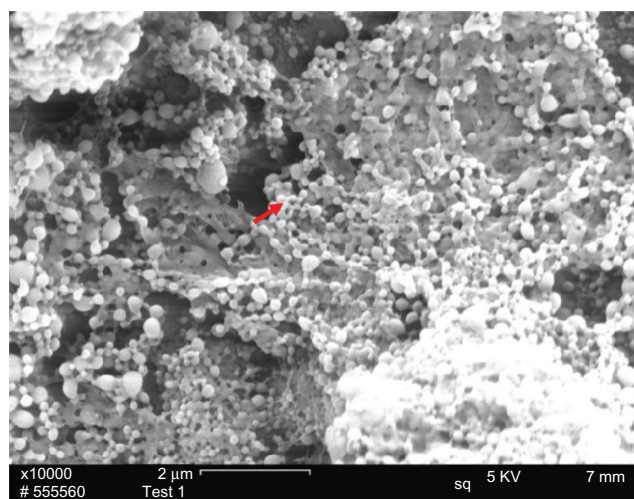
Figure 1 SEM imaging of PLNs.
Notes: PLN spheres were deposited on the surface of conductive carbon paper for SEM imaging. The red arrow refers to the PLN.
Abbreviations: SEM, scanning electron microscope; PLN, polymer–lipid nanoparticle.

mainly determined by the viscosity of both the organic phase and water phase used to prepare the nanoparticles.[28,29] The surfactants used for these two groups were Tween 80 for PLNs and PVA for the PLGA-NPs. Tween 80, with a much smaller molecular weight ([MW] 1310d) and lower used concentration (0.3 mg/mL) than the PVA (MW = 22 Kd, concentration 1%), produced less viscosity when dissolved in water and thus formed smaller particles during the nanoparticle-formation process. However, the encapsulation efficiency of PLN was 10% less than that of the PLGA-NPs, as shown in Table 1, probably because of the smaller size and lower emulsion capacity of Tween 80 compared with PVA. This result is consistent with the previous publication that nanoparticles with larger particle size tended to have higher drug-loading efficiency (probably due to less drug leakage in the fabrication process).[28] Zeta potential is a measure of the magnitude of the electrostatic, or charge, repulsion or attraction between particles.[30] As shown in Table 1, the Zeta potential results showed different surface properties for the two types of particles: a cationic surface for PLN, while anionic surface for the PLGA-NPs. It has been reported that the value of the

zeta potential affects the stability of the colloid system.[31] In Table 1, PLN possessed a higher value (46.5 mV), whereas PLGA-NPs possessed a lower value (15.5 mV), indicating that the PLN system was more stable than PLGA-NPs in terms of the resistance to coagulation.

Figure 2 shows an accumulative release of BSA profile from two groups of nanoparticles in vitro. An initial burst-release pattern was observed for PLGA-NPs. PLNs demonstrated a more sustained-release pattern compared with PLGA-NPs. The initial burst release from the PLGA-NPs may have been due to the fast release of the weakly absorbed BSA on the surface of nanoparticles. The lipid coating of the PLNs was helpful to stabilize the entrapped BSA and thus resulted in sustained release as expected. The specific mechanism for the interaction between polymers and proteins has not been elucidated so far, unfortunately.

Cellular uptake of PLGA-NPs and PLNs

As the predicate step of intracellular delivery of target protein, cellular uptake of the nanoparticles directly determined the further intracellular protein delivery efficacy. To evaluate the cellular internalization capacity of the nanoparticles, TR-BSA was used as a model drug. Three groups of samples, including TR-BSA-loaded PLGA-NPs, TR-BSA-loaded PLNs, and TR-BSA (control), were delivered to mouse fibroblasts within culture medium. Fluorescent microscope images in Figure 3 showed that TR-BSAs alone could hardly be detected within the cells, probably due to the degradation of protein in the cell culture
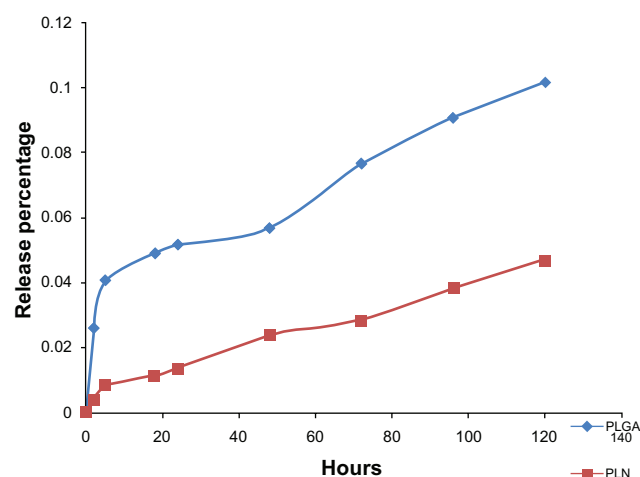
Table 1 The mean diameters and surface charge of PLNs and PLGA nanoparticles

Particle type	Size (nm)	Zeta potential (mV)	Encapsulation efficiency
PLNs	106.4 ± 30.2	46.5 ± 1.4	32.85% ± 1.89%
PLGA nanoparticles	209.8 ± 3.1	−15.5 ± 0.9	46.15% ± 3.78%

Abbreviations: PLN, polymer–lipid nanoparticle; PLGA, poly(lactic-co-glycolic) acid.

Figure 2 In vitro BSA release profile from PLGA-NPs and PLNs.
Notes: The profile in blue shows the BSA-release percentage from PLGA nanoparticles with initial burst release. The profile in red shows the BSA-release percentage from PLNs with a sustained-release pattern.
Abbreviations: BSA, bovine serum albumin; PLGA-NP, poly(lactic-co-glycolic) acid nanoparticle; PLN, polymer–lipid nanoparticle.
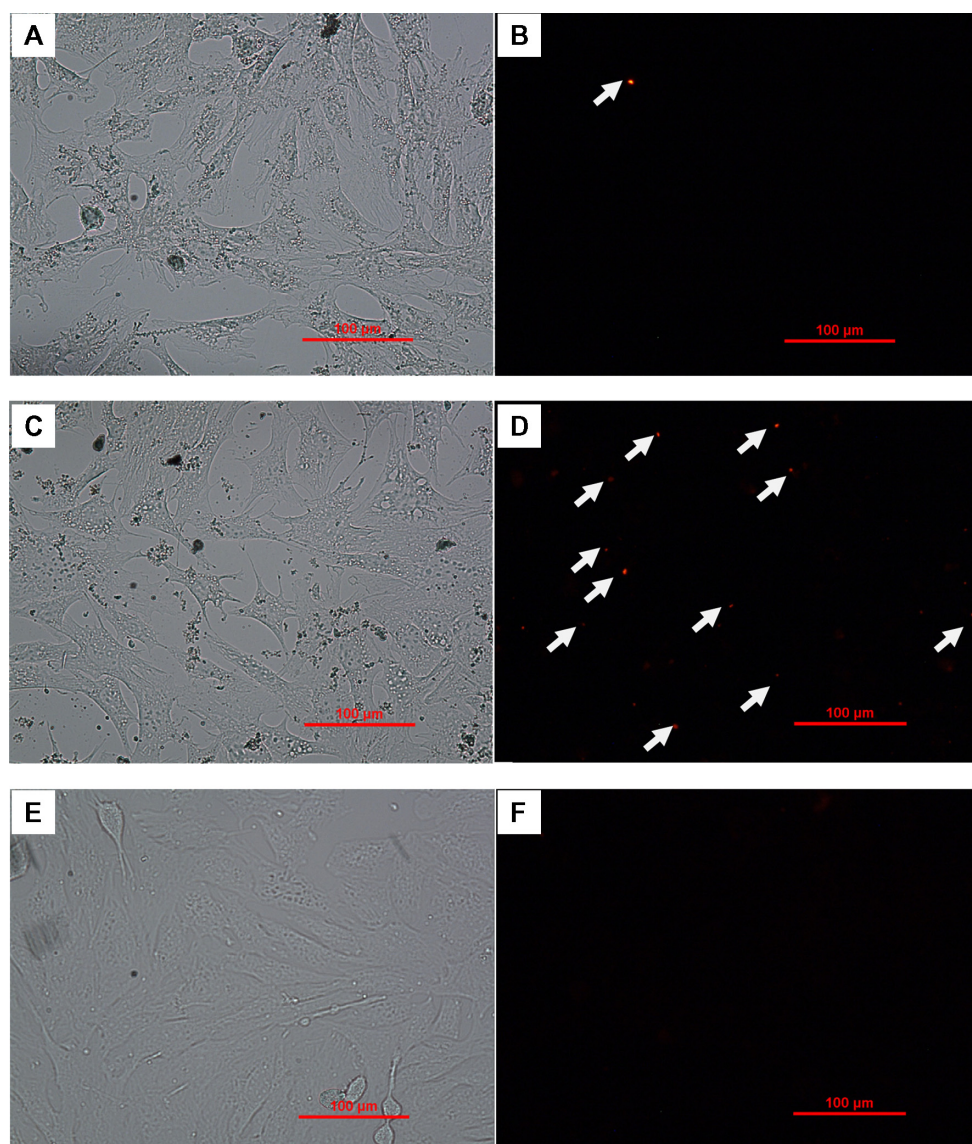
Figure 3 Cellular uptake of TR-BSA or TR-BSA-loaded particles after 4 hours incubation with medium, by mouse embryonic fibroblast cells.
Notes: (**A** and **B**) TR-BSA-loaded PLGA nanoparticles; (**C** and **D**): TR-BSA-loaded PLNs; (**E** and **F**): TR-BSA. (**A, C, E**) Bright field; (**B, D, F**) fluorescent red signal. The arrows refer to the fluorescent staining of TR-BSA in the nanoparticles.
Abbreviations: TR-BSA, Texas Red-labeled bovine serum albumin; PLGA, poly(lactic-co-glycolic) acid; PLN, polymer–lipid nanoparticle.

medium before cellular uptake. Both PLGA-NPs and PLNs demonstrated successful delivery of TR-BSA. However, there were more particles in the cells associated with the PLNs group than in cells associated with the PLGA-NPs group (Figure 3). One possible explanation is that more cells took up PLNs and that the internalized TR-BSAs in the PLNs remained stable in the cells after 4 hours. We speculate that either the slow protein release of the PLNs or the positive charge of the PLN outer layer may protect proteins from degradation in the endocytic vesicles or phagolysosomes. Therefore, in the following study, PLNs were the candidate intracellular delivery vehicle selected for further evaluation.

Intracellular protein targeting of PLNs

PLNs were next evaluated for antibody-directed intracellular targeting. Antibody against vinculin (a cytoplasmic protein that is associated with focal adhesions and actin cytoskeleton following fibroblast attachment to fibronectin)[32] was conjugated to PLNs carrying BSA as cargo. Vinculin antibody- or control antibody-conjugated PLNs were introduced into MEFs grown in fibrin–fibronectin gel culture. As shown in Figure 4, PLNs conjugated to either antibody were taken up by cells into the cytoplasm after one hour (Figure 4A–F). After 48 hours, most vinculin-targeting PLNs remained in the cytoplasm whereas a large fraction of control PLNs was, interestingly, localized in the nuclei (Figure 4G–L). Therefore,
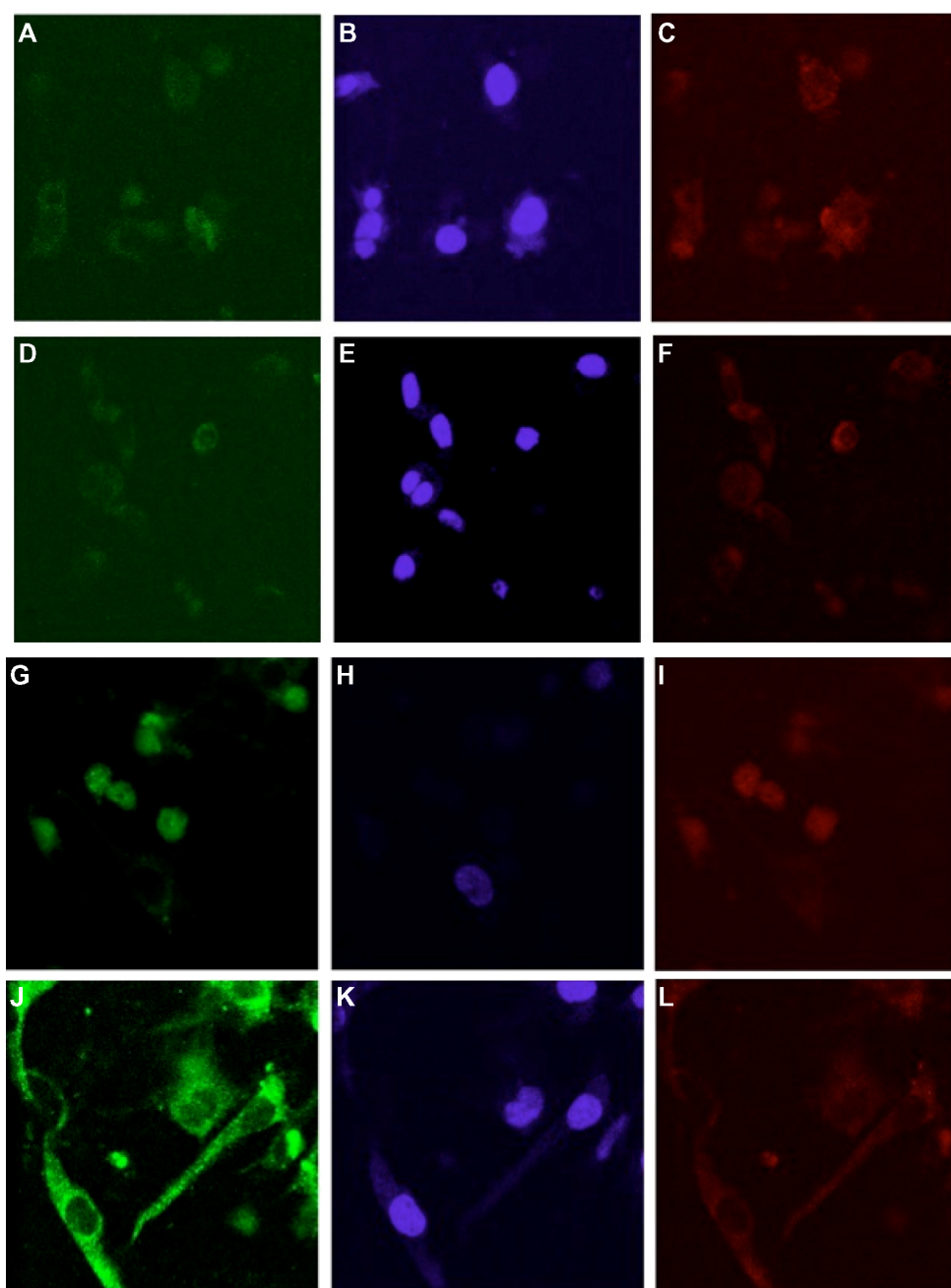
Figure 4 Vinculin-targeting nanoparticles in mouse embryo fibroblasts cultured in fibrin-fibronectin gel. Confocal fluorescent images of cells were taken after cells were incubated with PLNs for (**A**–**F**) 1 hour; (**G**–**L**) 48 hours. (**A** and **G**) PLNs labeled with control antibody conjugated to FITC; (**D** and **J**) PLNs labeled with FITC-anti-vinculin antibody; (**B**, **E**, **H**, and **K**) DAPI staining of cell nuclei; (**C**, **F**, **I**, and **L**) Texas Red-labeled BSA loaded to PLNs.
Abbreviations: PLN, polymer–lipid nanoparticle; FITC, fluorescein isothiocyanate; BSA, bovine serum albumin.

vinculin antibody conjugated to PLNs retained its function in the cellular environment for 48 hours and successfully targeted PLNs to the cytoplasm. Without targeting, internalized PLNs appear to have preferred nuclear localization. Although it is possible that the anti-vinculin antibody was partially digested after being incorporated within the cytoplasm, the remaining anti-vinculin antibody on the PLNs was still able to target the vinculin in the cytoplasm. As compared with

the controls, the strong fluorescent staining of cytoplasm by the anti-vinculin antibody-tagged PLNs group indicated their specificity (Figure 4). The anti-vinculin antibody was covalently conjugated onto PLNs, and the fluorescent staining was associated with PLNs. The specificity was further proved through the well-correlated distribution of embedded TR-BSA (Figure 4C, F, I, and L) in the PLNs in the cells with the fluorescent staining for antibody-FITC-PLNs in the
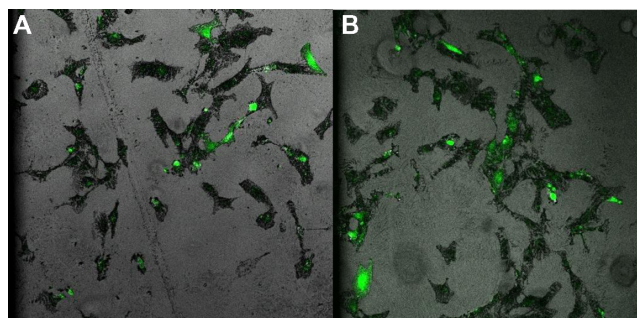
Figure 5 Confocal fluorescent microscopy of Hfob cells transfection with pIRES-EGFP after 24 hours by (**A**) Lipofectamine™ as the control; (**B**) PLN.
Abbreviations: Hfob, human osteoblast cells; PLN, polymer–lipid nanoparticle.

control and experimental groups (Figure 4A, D, J, and G). We then tested whether untargeted PLNs delivered cargo to the nuclei.

PLNs deliver plasmid DNA to the nucleus

To test the nuclear delivery of cargo, unconjugated PLNs were loaded with an expression vector pIRES-EGFP. Successful delivery of this vector to the nuclei and the structural integrity of the plasmid DNA during the delivery can be easily evaluated by the expression of a GFP reporter. The widely used commercial DNA transfection product, Lipofectamine 2000, was used as a control. Expressed GFP was visualized by confocal fluorescent microscope 24 hours after cellular uptake of PLNs as shown in Figure 5B. Compared with Lipofectamine 2000, the PLNs showed similar transfection efficiency (Figure 5). Therefore, the unconjugated PLNs without a nuclear localization signal can be used for nuclear targeting. DNA loaded in the PLNs remains stable in a cellular environment.

Conclusion

An intracellular protein-delivery vehicle was successfully fabricated from PLNs for controlled release of functional proteins. The PLNs exhibited stealth effect and could avoid the negative effect of serum on the cargo delivery to the intracellular compartment of cells. The anti-vinculin-conjugated PLNs were shown to be able to localize in cytoplasm. The unconjugated PLNs had nuclear-targeting capability in the absence of nuclear localization signals. By conjugating different targeting ligands, the PLNs could also potentially be used for delivery to other cellular organelles.

Acknowledgment

Disclosure

The authors report no conflicts of interest in this work.

References

1. Ruoslahti E, Bhatia SN, Sailor MJ. Targeting of drugs and nanoparticles to tumors. *J Cell Biol*. 2010;188(6):759–768.
2. Stadler A, Chi C, van der Lelie D, Gang O. DNA-incorporating nanomaterials in biotechnological applications. *Nanomedicine (Lond)*. 2010;5(2):319–334.
3. Ditto AJ, Shah PN, Yun YH. Non-viral gene delivery using nanoparticles. *Expert Opin Drug Deliv*. 2009;6(11):1149–1160.
4. Pan D, Caruthers SD, Chen J, et al. Nanomedicine strategies for molecular targets with MRI and optical imaging. *Future Med Chem*. 2010;2(3):471–490.
5. Gref R, Couvreur P, Barratt G, Mysiakine E. Surface-engineered nanoparticles for multiple ligand coupling. *Biomaterials*. 2003;24(24):4529–4537.
6. Calvo P, Remuñan-López C, Vila-Jato JL, Alonso MJ. Chitosan and chitosan/ethylene oxide-propylene oxide block copolymer nanoparticles as novel carriers for proteins and vaccines. *Pharm Res*. 1997;14(10):1431–1436.
7. Prabha S, Labhasetwar V. Critical determinants in PLGA/PLA nanoparticle-mediated gene expression. *Pharm Res*. 2004;21(2):354–364.
8. Breunig M, Bauer S, Goepferich A. Polymers and nanoparticles: intelligent tools for intracellular targeting? *Eur J Pharm Biopharm*. 2008;68(1):112–128.
9. Jiang J, Belikova NA, Hoye AT, et al. A mitochondria-targeted nitroxide/hemigramicidin S conjugate protects mouse embryonic cells against gamma irradiation. *Int J Radiat Oncol Biol Phys*. 2008;70(3):816–825.
10. Tomatsu S, Montaño AM, Dung VC, et al. Enhancement of drug delivery: enzyme-replacement therapy for murine Morquio A syndrome. *Mol Ther*. 2010;18(6):1094–1102.
11. Luzio JP, Parkinson MD, Gray SR, Bright NA. The delivery of endocytosed cargo to lysosomes. *Biochem Soc Trans*. 2009;37(Pt 5):1019–1021.
12. Hitoshi S, Yuichi S, Akira T, Isamu H. Importance of receptor-mediated endocytosis in peptide delivery and targeting: kinetic aspects. *Advanced Drug Delivery Reviews*. 1996;19(3):445–467.
13. Yan M, Du J, Gu Z, et al. A novel intracellular protein delivery platform based on single-protein nanocapsules. *Nat Nanotechnol*. 2009;5(1):48–53.
14. Panyam J, Zhou WZ, Prabha S, Sahoo SK, Labhasetwar V. Rapid endo-lysosomal escape of poly(DL-lactide-co-glycolide) nanoparticles: implications for drug and gene delivery. *FASEB J*. 2002;16(10):1217–1226.
15. He C, Hu Y, Yin L, Tang C, Yin C. Effects of particle size and surface charge on cellular uptake and biodistribution of polymeric nanoparticles. *Biomaterials*. 2010;31(13):3657–3666.
16. Mailänder V, Landfester K. Interaction of nanoparticles with cells. *Biomacromolecules*. 2009;10(9):2379–2400.
17. Xia T, Kovochich M, Liong M, et al. Polyethyleneimine coating enhances the cellular uptake of mesoporous silica nanoparticles and allows safe delivery of siRNA and DNA constructs. *ACS Nano*. 2009;3(10):3273–3286.
18. Tahara K, Sakai T, Yamamoto H, Takeuchi H, Hirashima N, Kawashima Y. Improved cellular uptake of chitosan-modified PLGA nanospheres by A549 cells. *Int J Pharm*. 2009;382(1–2):198–204.
19. Bieber T, Meissner W, Kostin S, Niemann A, Elsasser HP. Intracellular route and transcriptional competence of polyethylenimine-DNA complexes. *J Control Release*. 2002;82(2–3):441–454.
20. Merdan T, Kunath K, Fischer D, Kopecek J, Kissel T. Intracellular processing of poly(ethylene imine)/ribozyme complexes can be observed in living cells by using confocal laser scanning microscopy and inhibitor experiments. *Pharm Res*. 2002;19(2):140–146.

21. Tada S, Chowdhury EH, Cho CS, Akaike T. pH-sensitive carbonate apatite as an intracellular protein transporter. *Biomaterials*. 2010;31(6): 1453–1459.

22. Kuo KW, Chen TH, Kuo WT, Huang HY, Lo HY, Huang YY. Cell uptake and intracellular visualization using quantum dots or nuclear localization signal-modified quantum dots with gold nanoparticles as quenchers. *J Nanosci Nanotechnol*. 2010;10(7):4173–4177.

23. Mok H, Park TG. Direct plasmid DNA encapsulation within PLGA nanospheres by single oil-in-water emulsion method. *Eur J Pharm Biopharm*. 2008;68(1):105–111.

24. Michael KE, Dumbauld DW, Burns KL, Hanks SK, Garcia AJ. Focal adhesion kinase modulates cell adhesion strengthening via integrin activation. *Mol Biol Cell*. 2009;20(9):2508–2519.

25. Ziegler WH, Liddington RC, Critchley DR. The structure and regulation of vinculin. *Trends Cell Biol*. 2006;16(9):453–460.

26. Hinz B, Gabbiani G. Mechanisms of force generation and transmission by myofibroblasts. *Curr Opin Biotechnol*. 2003;14(5):538–546.

27. Yin Y, Chen D, Qiao M, Lu Z, Hu H. Preparation and evaluation of lectin-conjugated PLGA nanoparticles for oral delivery of thymopentin. *J Control Release*. 2006;116(3):337–345.

28. Dong Y, Feng SS. Methoxy poly(ethylene glycol)-poly(lactide) (MPEG-PLA) nanoparticles for controlled delivery of anticancer drugs. *Biomaterials*. 2004;25(14):2843–2849.

29. Wang J, Feng SS, Wang S, Chen ZY. Evaluation of cationic nanoparticles of biodegradable copolymers as siRNA delivery system for hepatitis B treatment. *Int J Pharm*. 2010;400(1–2):194–200.

30. Nash RA, Haeger BE. Zeta potential in the development of pharmaceutical suspensions. *J Pharm Sci*. 1966;55(8):829–837.

31. Kayes JB. Pharmaceutical suspensions: relation between zeta potential, sedimentation volume and suspension stability. *J Pharm Pharmacol*. 1977;29(4):199–204.

32. Humphries JD, Wang P, Streuli C, Geiger B, Humphries MJ, Ballestrem C. Vinculin controls focal adhesion formation by direct interactions with talin and actin. *J Cell Biol*. 2007;179(5):1043–1057.